Biochemical and Biophysical Research Communications 530 (2020) 665–672

Contents lists available at ScienceDirect

Biochemical and Biophysical Research Communications

journal homepage: www.elsevier.com/locate/ybbrc

Blocking sphingosine 1-phosphate receptor 2 accelerates hepatocellular carcinoma progression in a mouse model of NASH

Tomoaki Yoshida [a], Atsunori Tsuchiya [a, *], Masaru Kumagai [a], Suguru Takeuchi [a], Shunsuke Nojiri [a], Takayuki Watanabe [a], Masahiro Ogawa [a], Michiko Itoh [b], Masaaki Takamura [a], Takayoshi Suganami [c], Yoshihiro Ogawa [d], Shuji Terai [a, **]

[a] Division of Gastroenterology and Hepatology, Graduate School of Medical and Dental Sciences, Niigata University, 1-757, Asahimachi-dori, Chuo-ku, Niigata, 951-8510, Japan
[b] Kanagawa Institute of Industrial Science and Technology, 3-25-13, Tonomachi, Kawasaki-ku, Kawasaki, 210-0821, Japan
[c] Department of Molecular Medicine and Metabolism, Research Institute of Environmental Medicine, Nagoya University, Furu-cho, Chikusa-ku, Nagoya, 464-8601, Japan
[d] Department of Medicine and Bioregulatory Science, Graduate School of Medical Sciences, Kyushu University, 3-1-1, Maidashi, Higashi-ku, Fukuoka, 812-8582, Japan

ARTICLE INFO

Article history:
Received 19 July 2020
Accepted 22 July 2020
Available online 4 August 2020

Keywords:
JTE-013
S-adenosyl-L-methionine
Melanocortin-4 receptor
S1P-Specific G protein-coupled receptor 2
Glycine *N*-Methyltransferase

ABSTRACT

The role of sphingosine 1-phosphate (S1P) and its sphingosine-1-phosphate receptors (S1PRs) in non-alcoholic steatohepatitis (NASH) is unclear. We aimed to analyze the role of S1P/S1PRs in a Melanocortin-4 receptor (*Mc4r*)-deficient NASH murine model using FTY720, the functional antagonist of S1PR1, S1PR3, S1PR4, and S1PR5, and JTE-013, the antagonist of S1PR2. We observed that, compared to that in the control, the mRNA of *S1pr1* tended to decrease, whereas those of *S1pr2* and *S1pr3* significantly increased in *Mc4r*-knockout (KO) mice subjected to a Western diet (WD). While the fat area did not differ, fibrosis progression differed significantly between control mice and mice in which liver S1PRs were blocked. Lipidomic and metabolomic analysis of liver tissues showed that JTE-013-administered mice showed elevation of S-adenosyl-L-methionine level, which can induce aberrant methylation due to reduction in glycine *N*-methyltransferase (GNMT) and elevation in diacylglycerol (DG) and triacylglycerol (TG) levels, leading to increased susceptibility to hepatocellular carcinoma (HCC). These phenotypes are similar to those of *Gnmt*-KO mice, suggesting that blocking the S1P/S1PR2 axis triggers aberrant methylation, which may increase DG and TG, and hepatocarcinogenesis. Our observations that the S1P/S1PR2 axis averts HCC occurrence may assist in HCC prevention in NASH.

1. Introduction

Owing to the recent development of drugs for hepatitis B and C viruses, the prevalence of virus-related cirrhosis and hepatocellular carcinoma (HCC) is rapidly decreasing in developing countries. In contrast, non-alcoholic fatty liver disease (NAFLD) is becoming the major etiology of chronic liver diseases, in which patients with non-alcoholic steatohepatitis (NASH) are at high risk of developing liver fibrosis and HCC [1]. Along with the increase in the number of patients with NASH, lipid-related research, especially on sphingosine 1-phosphate (S1P), is also increasing.

S1P is a pluripotent bioactive signaling molecule generated by the phosphorylation of sphingosine by sphingosine kinase (SPHK) 1 and 2. S1P can bind and activate a family of five sphingosine-1-phosphate receptors (S1PR1–5), which can initiate a diverse range of cellular responses, including cell growth, survival, differentiation, migration, vascular integrity, lymphocyte trafficking, immune responses. The distribution of S1PRs is tissue-specific: for example, S1PR1–3 are expressed in various tissues including the liver; in contrast, the expression of S1PR4 and S1PR5 is restricted to specific organs but absent in the liver. In particular, S1PR4 is expressed in the lung, thymus, and spleen, while S1PR5 is expressed in the brain, skin, and spleen [2–4].

Reports show that, during disease progression in a mouse model

* Corresponding author. Niigata University, 1-757 Asahimachi-dori, Chuo-ku, Niigata, 951-8510, Japan.
** Corresponding author.
E-mail addresses: atsunori@med.niigata-u.ac.jp (A. Tsuchiya), terais@med.niigata-u.ac.jp (S. Terai).

https://doi.org/10.1016/j.bbrc.2020.07.099
0006-291X/

Abbreviations

S1P	sphingosine 1-phosphate
S1PR	sphingosine-1-phosphate receptor
NASH	non-alcoholic steatohepatitis
MC4R	melanocortin-4 receptor
HFD	high-fat diet
HCC	hepatocellular carcinoma
KO	knockout
SPHK	sphingosine kinase
GNMT	glycine *N*-methyltransferase
NAFLD	non-alcoholic fatty liver disease
WD	Western diet
SAMe	S-adenosyl-L-methionine
DG	diacylglycerol
TG	triacylglycerol
MCD	methionine-choline-deficient diet
ND	normal diet
PCR	polymerase chain reaction
PC	phosphatidylcholine
PEMT	phosphatidylethanolamine *N*-methyltransferase

of high-fat diet (HFD)-induced NAFLD, the S1P level increases in the liver [5]. Other studies have reported that the level of ceramide, the precursor of S1P, increases in NAFLD patients. These studies suggested that S1P played an important role in the pathophysiology of NAFLD [6]. Certain agonists, or antagonists, such as FTY720 and JTE-013, respectively, are used to analyze the role of the SPHK/S1P/S1PR axis in disease models [3,7,8]. FTY720, a substrate for SPHK, leads to the formation of phosphorylated FTY720, which competitively binds to S1PR1, 3, 4, and 5, resulting in their internalization and degradation, and eventually in the downregulation of S1PRs. Thus, FTY720 is a pharmacological agonist that acts as a functional antagonist by downregulating the S1P receptor. FTY720 is known to modulate the immune system by egressing lymphocytes from lymph nodes, and hence this drug is approved for treating multiple sclerosis [9]. JTE-013 is an S1PR2 antagonist; however, the role of S1PR2 has not been extensively investigated [8].

Melanocortin-4 receptor (*Mc4r*)-deficient mice fed HFD or Western diet (WD) are reported to act as a NASH mouse model with a phenotype similar to that of human NASH. MC4R is expressed in the hypothalamic nuclei and functions to regulate food intake and body weight; thus, this knockout (KO) mouse cannot control appetite and shows features similar to those observed in humans with NASH, such as obesity, insulin resistance, and liver steatosis. Steatohepatitis with fibrosis was observed 28 weeks after birth when HFD was started 8 weeks post-birth. In addition, HCC is often detected in this model approximately 1 year after birth. Thus, we can evaluate the effectiveness of certain drugs used for treating steatosis, fibrosis, and carcinogenesis in NASH using this mouse model [10–12].

In this study, we aimed to analyze the role of the SPHK/S1P/S1PR axis in steatosis, fibrosis, and carcinogenesis using *Mc4r*-KO NASH mouse model, and FTY720 and JTE-013.

2. Methods

2.1. Mice and diet

Mc4r-KO mice with a C57BL/6J background were provided by Joel K Elmquist (University of Texas Southern Medical Center, Dallas, TX, USA). Seven-week-old C57BL/6J male mice were purchased from Charles River (Yokohama, Japan). Individual cages housed four randomly selected mice in a 12-h day/night cycle, and the animals were allowed free access to food and water. All animal experiments were conducted in compliance with the regulations and approved by the Institutional Animal Care and Committee at the Niigata University.

We evaluated two different NASH mouse models: WD (Research Diets, Inc., New Brunswick, NJ, USA)-fed *Mc4r*-KO mice. Mice were fed with WD from 8 weeks of age and followed up to 6 weeks, 20 weeks, and 52 weeks after starting the WD. ND; CE-2, CLEA Japan, Inc., Tokyo, Japan)-fed *Mc4r*-KO mice were used as the control group. (Supplemental Fig. 1).

2.2. FTY720 and JTE-013

To identify the role of S1PRs in NASH, we used FTY720/fingolimod (Cayman Chemical, Ann Arbor, MI, USA) as a functional antagonist that binds to four of the S1P receptors (S1PR1, S1PR3, S1PR4, and S1PR5) and JTE-013 (Cayman Chemical) as the antagonist of S1PR2. After feeding mice WD for 16 weeks, therapy with FTY720, JTE-013, or vehicle was performed for 4 weeks. FTY720 and JTE-013 were administered intraperitoneally at 10 mg/kg twice a week for 4 weeks. The mice were analyzed after eight injections (Supplemental Fig. 2).

2.3. Statistical analysis

Statistical analysis was performed using the GraphPad Prism6 software (GraphPad Software Inc., La Jolla, CA, USA). Data have been presented as the mean ± standard deviation. The results were assessed using the Student's *t*-test. Differences between groups were analyzed using one-way analysis of variance. Differences were considered significant when $P < 0.05$.

Further description of the materials and methods used are provided in supplemental information.

3. Results

3.1. Expression pattern of S1P receptors and Sphk during the development of steatohepatitis

Initially, we analyzed the mRNA expression pattern of *S1pr*1–3 and *Sphk*s using *Mc4r*-KO mouse. WD was started from 8 weeks of age, and the mice were analyzed 20 weeks later. Animals of the same age on a normal diet (ND) were compared (Supplemental Fig. 1). In this study, *S1pr1* expression tended to decrease ($P = 0.13$), while *S1pr2* ($P = 0.03$) and *S1pr3* ($P = 0.04$) expression increased significantly compared to that of the control. Although the *Sphk1* expression was significantly higher than that in the control ($P < 0.01$), *Sphk2* expression did not change significantly ($P = 0.23$) (Fig. 1A). Next, we analyzed the expression pattern of *S1pr*s and *Sphk*s for 1 year. During the follow-up, *S1pr1* expression decreased significantly; in contrast, *S1pr2* expression increased significantly ($P < 0.05$), whereas that of *S1pr3* did not change appreciably. *Sphk1* expression increased significantly with time, whereas that of *Sphk2* decreased significantly ($P < 0.01$) (Fig. 1B). These results showed that during NASH development, S1P production and the expression pattern of *S1pr*s changed significantly, which implied that S1PR1-and S1PR2-related signals were important for the pathophysiology of NASH.

Blocking of S1P by FTY720 and JTE-013 Tended to Deteriorate Liver Damage and Fibrosis Progression.

To analyze the role of S1PR1–3 in *Mc4r*-KO mice, we used FTY720, which can block all signals except for S1PR2, and JTE-013, which blocks S1PR2. *Mc4r*-KO mice were fed with ND or WD from 8

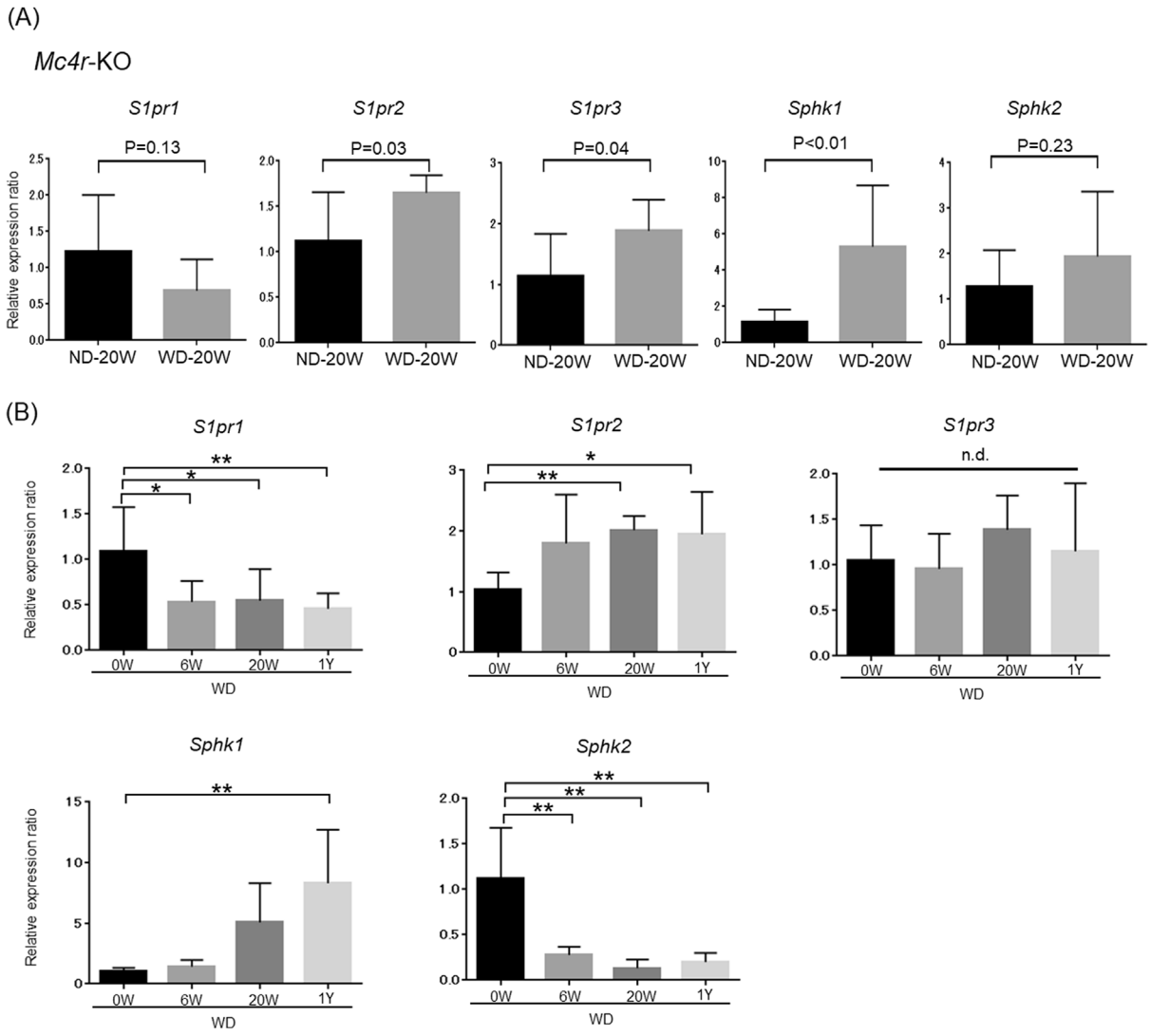

Fig. 1. Expression pattern of S1P receptors and sphingosine kinases (*Sphks*) during the development of steatohepatitis in different non-alcoholic steatohepatitis mouse models. Data have been presented as means ± standard deviation. (A) Changes in the mRNA expression pattern in *Mc4r*-KO mice fed with WD (ND; n = 8, WD; n = 7) compared to control mice. (B) mRNA expression changes with time in *Mc4r*-KO mice fed with WD (n = 4–7) (*P < 0.05, **P < 0.01, n.d. no significant difference).

weeks after birth and were analyzed 20 weeks later; during the last 4 weeks, vehicle (WD-vehicle), FTY720, or JTE-013 were administered intraperitoneally twice a week in the WD groups (Supplemental Fig. 2). Mice fed with WD tended to have high liver-to-body weight ratio and serum levels of aspartate transaminase, alanine transaminase, and total cholesterol. Mice in the JTE-013 and FTY720 groups tended to have high serum levels of aspartate transaminase (AST) and alanine transaminase (ALT), which, however, was not significant compared to that of the WD-vehicle group (Fig. 2A). Real-time Polymerase Chain Reaction (PCR) analysis using liver tissues revealed that mice fed with WD also tended to have high levels of inflammatory cytokines and growth factors such as *Il6*, *Tnfa*, and *Tgfb*, and chemokines such as *Cxcl2*, *Ccl2*, and *Cxcr4*. Mice in the JTE-013 and FTY720 groups tended to express high levels of *Tnfa*, *Tgfb*, *Cxcl2*, *Ccl2*, and *Cxcr4* in the liver, which, however, was not significant compared to that in the WD-vehicle group (Supplemental Fig. 3). These results showed that mice in the WD group, especially those subjected to JTE-013 and FTY720 treatment, tended to show high levels of inflammation. Next, fat accumulation in the liver was evaluated by calculating the fat area in the liver tissue; however, we did not detect any significant difference in fat accumulation in these tissues (Fig. 2B and E). However, the number of hepatic crown-like structure (hCLS), which is F4/80+ and is involved in the development of hepatic inflammation and fibrosis in *Mc4r*-KO mice fed with a WD, and TUNEL + cells were significantly increased in the JTE-013 and FTY720 groups compared to that in the WD-vehicle group (P < 0.01) (Fig. 2C and F and Supplemental Fig. 4) [13]. Finally, fibrosis was evaluated using Sirius Red staining and real-time PCR on liver tissues. Samples from both JTE-013 and FTY720 groups showed higher fibrosis area than those from the WD-vehicle group after Sirius Red staining (P < 0.01) (Fig. 2D and G), and the same tendency was observed in the real-time PCR analysis of *Timp1*, *Mmp2,* and *Col1a1* (Supplemental Fig. 5). These results demonstrated that, although not all differences were statistically significant, blockade of the SPHK/S1P/S1PR axis tended to adversely affect liver inflammation and fibrosis.

3.2. Blocking of S1PR2 by JTE-013 increased susceptibility to HCC

Next, we analyzed tumor formation using the same model, as mentioned above. Intriguingly, tumor formation was observed only

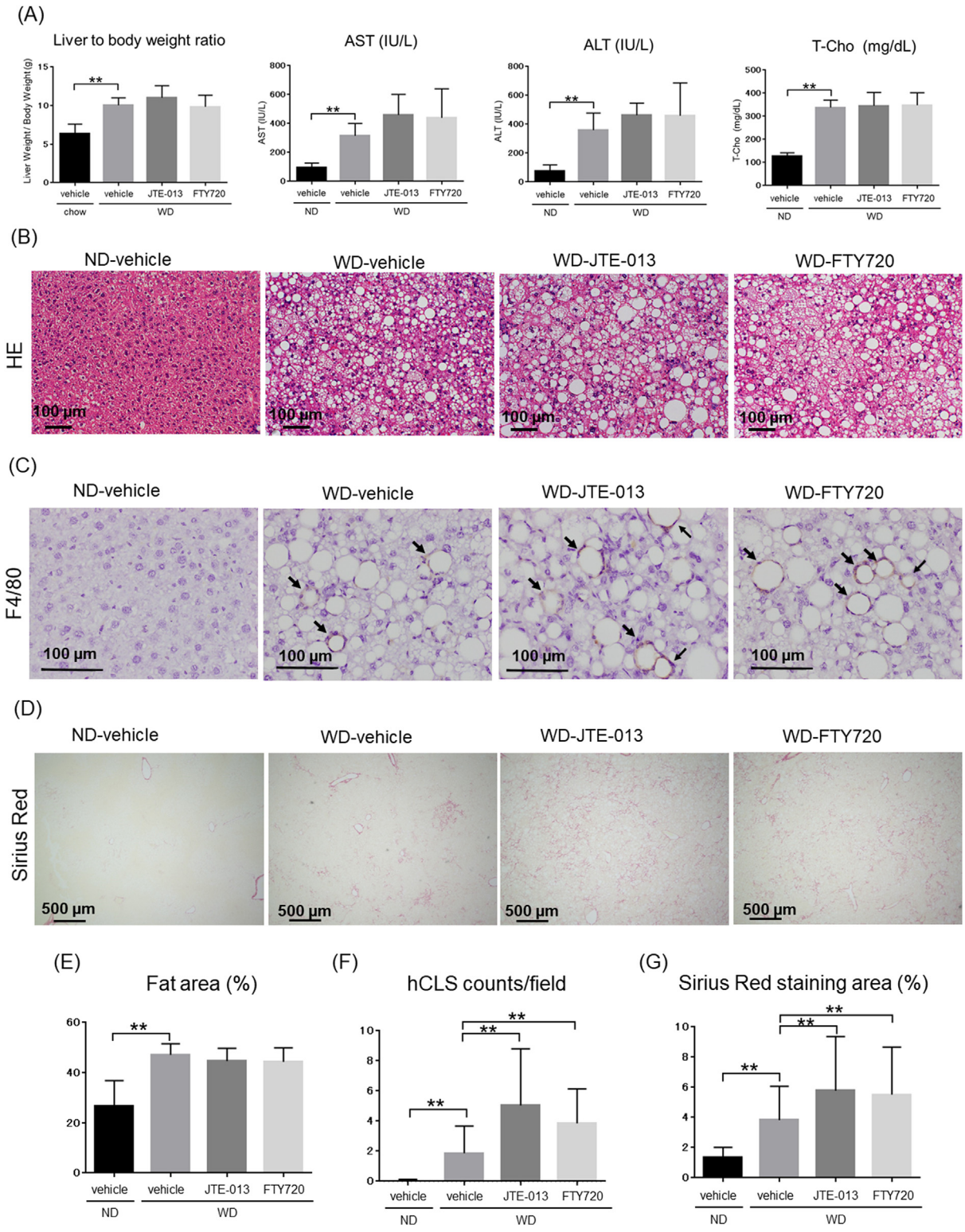

Fig. 2. Therapeutic effect of FTY720 and JTE-013 in WD-fed *Mc4r*- KO mice. Data have been presented as means ± standard deviation. (A) Liver-to-body weight ratio and serum levels of aspartate transaminase (AST), alanine transaminase (ALT), and total cholesterol (T-Cho) were analyzed. (B) Hematoxylin and eosin staining (scale bar: 100 μm) and (C) Immunohistochemical analyses for F4/80 have been shown (scale bar: 100 μm). Black arrows reveal hepatic crown-like structures (hCLS). (D) Sirius Red staining (scale bar: 500 μm). (E) Fat accumulation in the liver evaluated by calculating the area of fat in the liver tissue. (n = 7–8) (F) Number of hCLS. (n = 7–8) (G) The frequency of occurrence of Sirius Red-stained area were analyzed using Image J (n = 7–8) (*P < 0.05, **P < 0.01). (For interpretation of the references to colour in this figure legend, the reader is referred to the Web version of this article.)

in the JTE-013 group (3 of 8 mice, 37.5%) but not in other groups, including the FTY720 group (Fig. 3A). One tumor was formed per mouse, and tumors were not observed in other organs. Pathological analysis of the tumor revealed fat accumulation, and the tumor was similar to well-differentiated HCC (Fig. 3B). We also evaluated the cell growth potential using Ki-67 staining; results showed that the number of Ki-67+ tumor cells was approximately 20 cells/field and was significantly higher than that in non-tumor cells (Fig. 3C). Thus, blocking S1PR2 with JTE-013 increased the susceptibility to HCC. To further analyze the mechanisms underlying this phenomenon, lipidomics and metabolomics analyses were performed using individual liver tissues.

Blocking of S1PR2 by JTE-013 Showed the Same Phenotype as That in *Gnmt*-KO Mice.

(A)

Diet		Chow	Western diet		
i.p.		Vehicle (n = 8)	Vehicle (n = 7)	JTE-013 (n = 8)	FTY720 (n = 7)
Tumor	+	0	0	3	0
	—	8	7	5	7

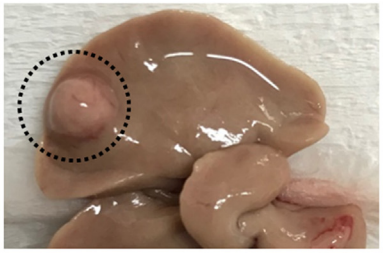

(B)

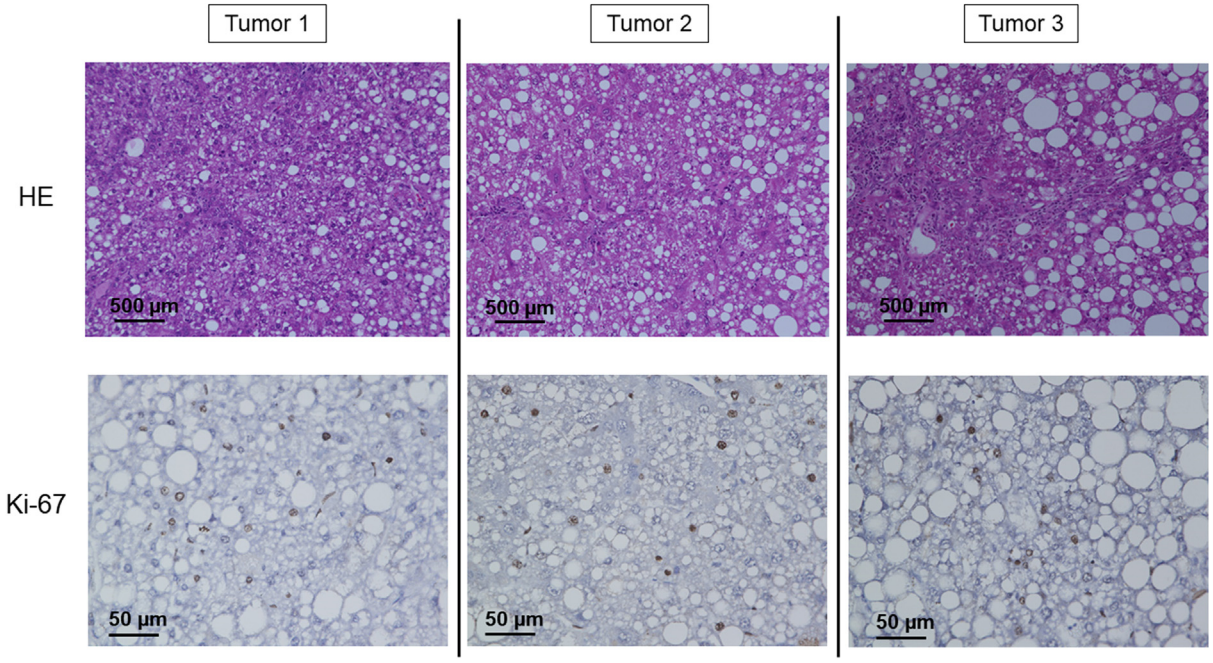

(C) Ki-67 staining

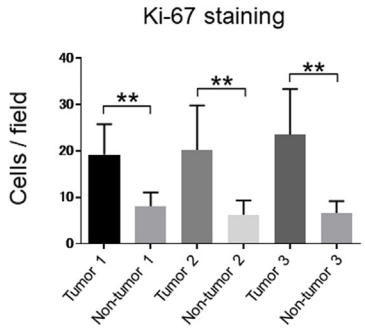

Fig. 3. Hepatocellular carcinoma (HCC) after FTY720 or JTE-013 administration. Data have been presented as means ± standard deviation. (A) The number of mice with HCC was calculated. (B) Hematoxylin and eosin (HE) staining and immunohistochemical analysis for Ki-67 have been shown (Upper panels; HE staining, lower panels; Ki-67 staining, scale bar: 500 μm). (C) Number of immune-positive cells for Ki-67 in the tumor area and non-tumor area have been shown (**P < 0.01). i.p., intraperitoneal.

First, lipidomics was performed to analyze the lipid profile. The differences between the two groups were analyzed using a differential map. Compared to ND-control mice, a wide range of changes were observed in *Mc4r*-KO mice fed with WD. In WD-fed mice, the FTY720 group and WD-control group did not differ significantly; however, the JTE-013 and WD-control groups, especially the JTE-013 and FTY720 groups, differed considerably (Supplemental Fig. 6). The heat map and metabolic map revealed that mainly diacylglycerol (DG) and some triacylglycerol (TG) accumulated in the liver (Fig. 4A). For example, a comparison of the JTE-013 group with the FTY720 group revealed that the levels of DG (38:4), arachidonate (20:4), and DG (38:3) had increased (Supplemental Fig. 7). These results revealed that the lipid content, mainly those of DG and TG, in the liver, were increased by blocking the SPHK/S1P/S1PR2 axis.

Next, we performed a metabolomics analysis. We observed that the S-adenosyl-L-methionine (SAMe) level had increased, and that of S-adenosyl-L-homocysteine had decreased in the JTE-013 group (Fig. 4B). The first step in mammalian methionine metabolism is the conversion to SAMe and transfer of the methyl group of SAMe to various substances, such as DNA, RNA, histones, and small molecules such as glycine, guanidinoacetate, and phosphatidylethanolamine, with the formation of S-adenosyl-L-homocysteine. S-adenosyl-L-homocysteine is an inhibitor of many SAMe-dependent methyltransferases. Glycine *N*-methyltransferase (GNMT) is one of the key enzymes involved in methionine and SAMe metabolism, and *Gnmt*-KO mice, characterized by highly elevated SAMe and methionine levels, have been reported to develop steatosis, fibrosis, and HCC [14,15]. As the SAMe level had increased and the S-adenosyl-L-homocysteine level had decreased in the JTE-013 group, and liver tumor formation was observed only in this group, we suspected that GNMT levels in this group would be low. Thus, Western blot analysis was performed, and, expectedly, the GNMT levels in the liver of the JTE-013 group were low (Fig. 4C). These results suggested that blocking the SPHK/S1P/S1PR2 axis increased the susceptibility to HCC by decreasing the GNMT level. Martínez-Uña et al. reported that, when hepatic SAMe accumulation occurs in *Gnmt*-KO mice, an adaptive route of phosphatidylcholine (PC) synthesis via the phosphatidylethanolamine *N*-methyltransferase (PEMT) pathway was stimulated to reduce SAMe, and the excess DG generated was catabolized, leading to TG synthesis and steatosis [15]. Thus, we determined the status of PC and phosphatidylethanolamine (PE) in the JTE-013 group and found that PC/PE ratio in the liver tended to increase in the JTE-013 group as compared to other groups (Supplemental Fig. 8, Supplemental Fig. 9). All these results revealed that blocking S1PR2 with JTE-013 promoted a phenotype similar to that observed in *Gnmt*-KO mice (Fig. 4D).

4. Discussion

This study provides the first evidence connecting the blockage of the SPHK/S1P/S1PR2 axis to SAMe elevation, which is involved in methionine metabolism. The following occurred when the SPHK/S1P/S1PR2 axis was blocked in the NASH mouse (*Mc4r*-KO) model: 1) DG and TG levels increased in liver tissues, as observed using lipidomics; 2) SAMe level was increased, and GNMT level was decreased in the liver tissues, as observed using metabolomics and western blotting, respectively; and 3) susceptibility to HCC increased, as observed using liver histology. These results corroborated the previously reported phenotype of *Gnmt*-KO mice, in which SAMe accumulation was observed, resulting in aberrant methylation due to the lack of catalysis of SAMe by GNMT, and subsequently increasing the susceptibility to HCC. Reports show that GNMT is absent in HCC, and its mRNA levels are significantly lower in the livers of patients at risk of developing HCC; hence, GNMT has been proposed to be a tumor susceptibility gene for liver cancer [14,15]. Furthermore, as an adaptive response to hepatic SAMe accumulation, PC synthesis via the PEMT pathway is stimulated, and the excess DG generated is catabolized in this *Gnmt*-KO mouse, leading to TG synthesis and steatosis (Fig. 4E; highlight). GNMT protein may be downregulated when liver damage occurs. In this study, we showed that *Mc4r*-KO mice in the FTY720 group had nearly the same levels of liver damage (transaminase levels, area of fat in the liver, and frequency of fibrosis area) as those in the JTE-013 group; however, the GNMT levels and lipid contents and occurrence of HCCs clearly differed between these groups. Thus, liver damage alone did not determine the levels of GNMT, and the difference was caused by differences in the FTY720 and JTE-013 groups (the signals of S1P/S1PR axis). These observations clearly show the new interface between the SPHK/S1P/S1PR axis and cancer progression in NASH, which will be beneficial for preventing steatosis and cancer in the future.

Recently, the pathobiology of S1P is being extensively investigated for identifying new therapeutic targets in acute and chronic liver diseases, including NAFLD. The role of S1P in acute and chronic liver disease is controversial. Although many studies have suggested that S1P contributes to liver damage by recruiting and activating the immune cells that cause it, some studies have demonstrated its protective role in hepatocyte apoptosis [16,17]. Several papers have also analyzed the specific role of S1PRs using FTY720 and JTE-013 in models of acute and chronic liver damage. S1PR1 is often reported to be related to the regulation of trafficking and activation of immune cells. Kaneko et al. reported that FTY720 and KRP203, functional antagonists of S1PR1, protected from concanavalin-A-mediated T cell-dependent acute liver injury by reducing the recruitment of inflammatory cells [18]. Another study reported that FTY720 reduced the liver/body weight ratio along with hepatic inflammation, fibrosis, and hepatocyte ballooning in the NAFLD mouse model [9], indicating that FTY720 played a protective role. However, in our study, 4 weeks of administration of FTY720 did not improve liver inflammation, steatosis, and fibrosis. Hence, we assumed that 4 weeks of FTY720 administration were not sufficient to observe the abovementioned effect. In addition, these differences might have arisen due to variations in the mouse model used. We believe that further studies custom-designed for the situation are required to determine the role of S1PR1 or FTY720 in liver diseases. Compared to studies on S1PR1, those on S1PR2 are limited in number. Wang et al. reported that, when S1PR2 was blocked using JTE-013 in the CCl4-induced liver fibrosis model, a significant attenuation of serum ALT levels, exosome number, collagen I mRNA expression, Sirius Red staining, and α-smooth muscle actin and collagen I protein expression was observed in the liver tissue compared to that in mice treated with CCl4 alone [19]. Another study reported that, in a bile duct ligation-induced liver fibrosis model, JTE-013 significantly reduced total bile acid levels after serum and cholestatic liver injury [20]. In our study, we did not observe the protective effect, which, however, might be due to the mouse model used. Nagahashi et al. reported the expression of genes encoding S1PR2 in primary mouse hepatocytes differentially upregulated genes encoding enzyme/nuclear receptors involved in sterol and lipid metabolism. Both *S1pr2*-KO and *Sphk2*-KO mice rapidly developed fatty livers on HFD with an accumulation of cholesterol and TG. Furthermore, they observed that both *S1pr2*-KO and *Sphk2*-KO mice on ND also accumulated lipids in the liver, although to a considerably lesser extent than those in mice on HFD.

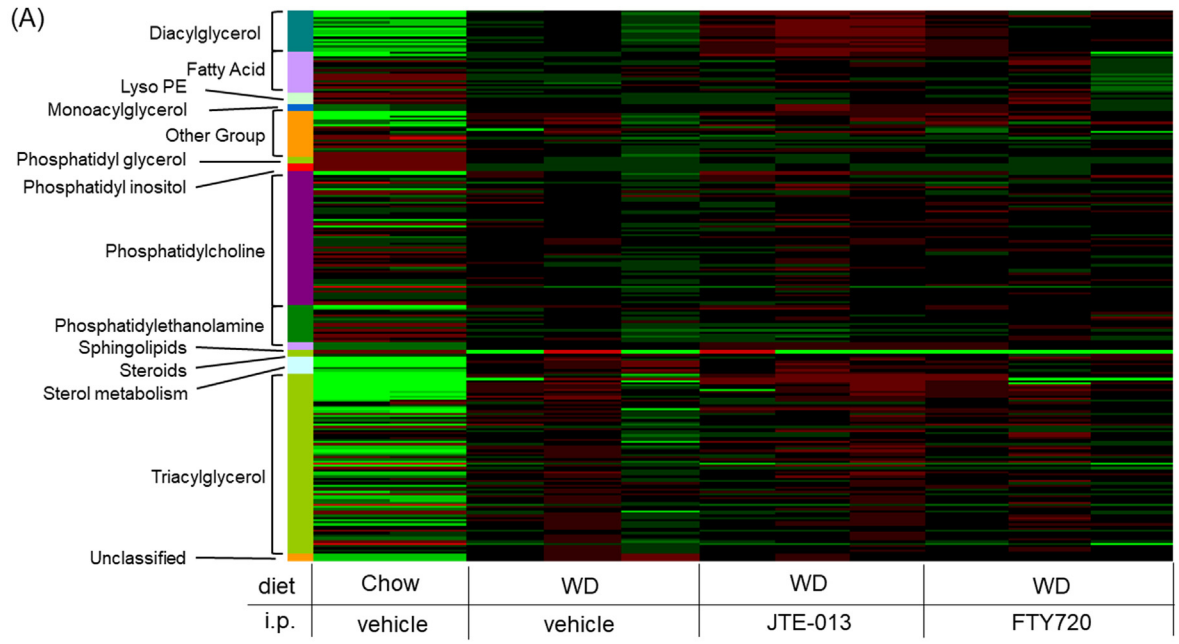

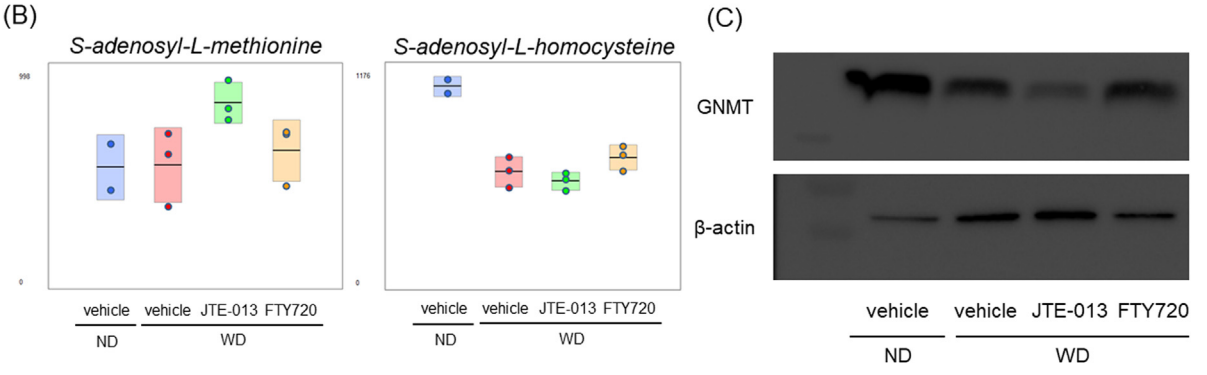

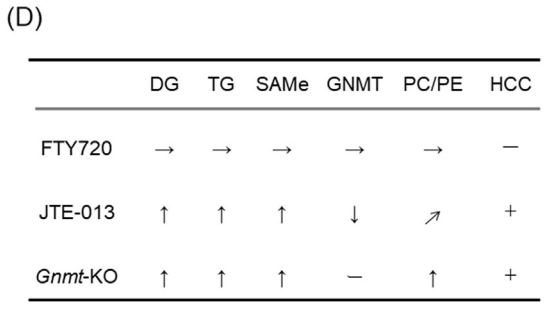

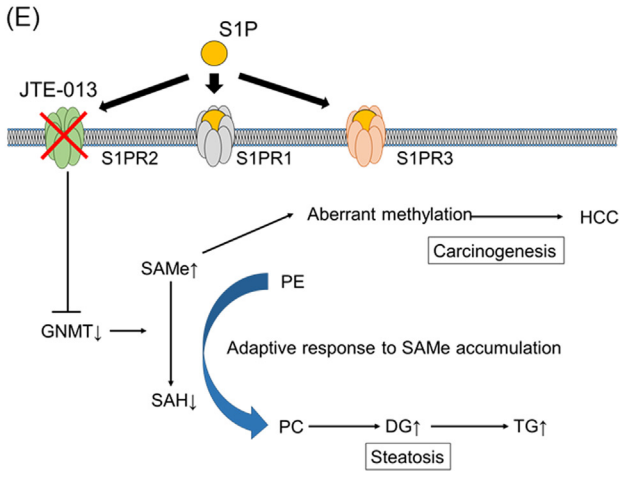

Fig. 4. Changes in the lipid component of the liver were analyzed using lipidomics and the metabolic pathway in the liver were analyzed using metabolomics and after FTY720 or JTE-013 administration. (A) Heat map from lipidomics data analysis. Red indicates that the metabolite content is relatively high, whereas green indicates that it is low. i.p., intraperitoneal. (B) Box plot analysis of metabolomics showing changes in S-adenosyl-L-methionine and S-adenosyl-L-homocysteine. (C) Representative Western blot analysis of glycine *N*-methyltransferase (GNMT). (D) Comparison between our data and data of *Gnmt*-KO mouse has been shown. (E) Schematic showing the highlights of this study obtained from our results regarding the mechanism underlying the development of HCC after the sphingosine-1-phosphate receptor (S1PR) 2 blockage. SAMe, S-adenosyl-L-methionine; SAH, S-adenosyl-L-homocysteine; DG, diacylglycerol; TG, triacylglycerol. (For interpretation of the references to colour in this figure legend, the reader is referred to the Web version of this article.)

They speculated that the genes involved in the transport and metabolism of lipids (i.e., *Apob* and *Cpt1a*) were not upregulated in the liver of *Sphk2*-or *S1pr2*-deficient animals, leading to fatty liver development [21]. Our study also suggests that blocking S1PR2 with JTE-013 in *Mc4r*-KO mice resulted in the accumulation of DG and TG in the liver. This observation, together with the results of Nagahashi et al. suggests that the SPHK/S1P/S1PR2 axis can be a target for the treatment of liver steatosis.

The function of S1P, which is related to cell proliferation, differentiation, angiogenesis, chemotaxis, and migration, is naturally related to cancer biology. Each of these S1PRs appears to be tissue-specific and has demonstrated to be involved in the regulation of cell proliferation and survival in various cancer types.

The roles of S1PR2 in cancer remain controversial. S1PR2 has been reported to act both as anti- and pro-cancer receptor. For instance, in melanoma, glioblastoma, and B-cell lymphoma, S1PR2 acts as an anticancer receptor. On the other hand, the role of S1PR2 as a carcinogenic receptor has been reported in prostate cancer. A review on the role of S1PR2 in cancer mentions that the effect of this receptor on tumor growth and progression is cell type-specific, possibly due to its coupling with particular G proteins, which regulates biological functions [22]. Thus, despite the context-specific, controversial evidence, we report the anticancer receptor activity of S1PR2 in the liver of the NASH mice. Although we did not detect cancer in other organs, we shall investigate further the occurrence of cancer in other organs.

The main limitation of this study was that, although our findings supported the previously reported phenotype of the *Gnmt*-KO mouse, which showed SAMe accumulation and aberrant methylation due to the lack of the SAMe catalysis by GNMT, resulting in increased susceptibility to HCC, we could not identify the pathway connecting S1PR2 and GNMT downregulation.

This study provides the first evidence connecting the blockage of the SPHK/S1P/S1PR2 axis with the acceleration of the occurrence of HCC. We believe that our findings on the antioncogenic activity of S1PR2 receptor will pave the way for the identification of target drugs to reduce the occurrence of HCC among patients with NAFLD.

Disclosures

The authors declare no conflict of interest.

Author contributions

TY and AT proposed the study and drafted the manuscript. TY, AT, MK, SG-T, SN, TW, MO, MI and MT performed the experiments. TS, YO and SH-T provided critical comments and edits to the manuscript. All authors approved the final version of the manuscript.

Financial support

This research was supported by a Grant-in-Aid for Scientific Research (B) (19H03636) from the Ministry of Education, Culture, Sports, Science and Technology of Japan.

Declaration of competing interest

The authors declare that they have no known competing financial interests or personal relationships that could have appeared to influence the work reported in this paper.

Acknowledgments

We thank Takao Tsuchida for his cooperation in the preparation of pathological tissue.

Appendix A. Supplementary data

Supplementary data to this article can be found online at https://doi.org/10.1016/j.bbrc.2020.07.099.

References

[1] Z.M. Younossi, A.B. Koenig, D. Abdelatif, et al., Global epidemiology of nonalcoholic fatty liver disease-Meta-analytic assessment of prevalence, incidence, and outcomes, Hepatology 64 (2016) 73–84.
[2] M.J. Kluk, T. Hla, Signaling of sphingosine-1-phosphate via the S1P/EDG-family of G-protein-coupled receptors, Biochim. Biophys. Acta 1582 (2002) 72–80.
[3] T. Rohrbach, M. Maceyka, S. Spiegel, Sphingosine kinase and sphingosine-1-phosphate in liver pathobiology, Crit. Rev. Biochem. Mol. Biol. 52 (2017) 543–553.
[4] I. Ishii, B. Friedman, X. Ye, et al., Selective loss of sphingosine 1-phosphate signaling with no obvious phenotypic abnormality in mice lacking its G protein-coupled receptor, LP(B3)/EDG-3, J. Biol. Chem. 276 (2001) 33697–33704.
[5] A.J. Sanyal, T. Pacana, A lipidomic readout of disease progression in A diet-induced mouse model of nonalcoholic fatty liver disease, Trans. Am. Clin. Climatol. Assoc. 126 (2015) 271–288.
[6] G. Grammatikos, C. Muhle, N. Ferreiros, et al., Serum acid sphingomyelinase is upregulated in chronic hepatitis C infection and non alcoholic fatty liver disease, Biochim. Biophys. Acta 1841 (2014) 1012–1020.
[7] B. Gonzalez-Fernandez, D.I. Sanchez, J. Gonzalez-Gallego, et al., Sphingosine 1-phosphate signaling as a target in hepatic fibrosis therapy, Front. Pharmacol. 8 (2017) 579.
[8] M. Adada, D. Canals, Y.A. Hannun, et al., Sphingosine-1-phosphate receptor 2, FEBS J. 280 (2013) 6354–6366.
[9] A.S. Mauer, P. Hirsova, J.L. Maiers, et al., Inhibition of sphingosine 1-phosphate signaling ameliorates murine nonalcoholic steatohepatitis, Am. J. Physiol. Gastrointest. Liver Physiol. 312 (2017) G300–G313.
[10] M. Itoh, T. Suganami, N. Nakagawa, et al., Melanocortin 4 receptor-deficient mice as a novel mouse model of nonalcoholic steatohepatitis, Am. J. Pathol. 179 (2011) 2454–2463.
[11] M. Itoh, T. Suganami, H. Kato, et al., CD11c+ resident macrophages drive hepatocyte death-triggered liver fibrosis in a murine model of nonalcoholic steatohepatitis, JCI Insight (2017) 2.
[12] C. Komiya, M. Tanaka, K. Tsuchiya, et al., Antifibrotic effect of pirfenidone in a mouse model of human nonalcoholic steatohepatitis, Sci. Rep. 7 (2017) 44754.
[13] M. Itoh, H. Kato, T. Suganami, et al., Hepatic crown-like structure: a unique histological feature in non-alcoholic steatohepatitis in mice and humans, PloS One 8 (2013), e82163.
[14] M.L. Martinez-Chantar, M. Vazquez-Chantada, U. Ariz, et al., Loss of the glycine N-methyltransferase gene leads to steatosis and hepatocellular carcinoma in mice, Hepatology 47 (2008) 1191–1199.
[15] M. Martinez-Una, M. Varela-Rey, A. Cano, et al., Excess S-adenosylmethionine reroutes phosphatidylethanolamine towards phosphatidylcholine and triglyceride synthesis, Hepatology 58 (2013) 1296–1305.
[16] Y. Osawa, H. Uchinami, J. Bielawski, et al., Roles for C16-ceramide and sphingosine 1-phosphate in regulating hepatocyte apoptosis in response to tumor necrosis factor-alpha, J. Biol. Chem. 280 (2005) 27879–27887.
[17] T. Nowatari, S. Murata, K. Nakayama, et al., Sphingosine 1-phosphate has anti-apoptotic effect on liver sinusoidal endothelial cells and proliferative effect on hepatocytes in a paracrine manner in human, Hepatol. Res. 45 (2015) 1136–1145.
[18] T. Kaneko, T. Murakami, H. Kawana, et al., Sphingosine-1-phosphate receptor agonists suppress concanavalin A-induced hepatic injury in mice, Biochem. Biophys. Res. Commun. 345 (2006) 85–92.
[19] R. Wang, Q. Ding, U. Yaqoob, et al., Exosome adherence and internalization by hepatic stellate cells triggers sphingosine 1-Phosphate-dependent migration, J. Biol. Chem. 290 (2015) 30684–30696.
[20] Y. Wang, H. Aoki, J. Yang, et al., The role of sphingosine 1-phosphate receptor 2 in bile-acid-induced cholangiocyte proliferation and cholestasis-induced liver injury in mice, Hepatology 65 (2017) 2005–2018.
[21] M. Nagahashi, K. Takabe, R. Liu, et al., Conjugated bile acid-activated S1P receptor 2 is a key regulator of sphingosine kinase 2 and hepatic gene expression, Hepatology 61 (2015) 1216–1226.
[22] N.J. Pyne, A. El Buri, D.R. Adams, et al., Sphingosine 1-phosphate and cancer, Adv. Biol. Regul. 68 (2018) 97–106.